Superconductivity and Cryogenics
Vol.12, No.4, (2010), pp.24~30

Feasibility study on the design of DC HTS cable core

Kideok Sim[1,*], Seokho Kim[2], Hyun-man Jang[3], Su-kil Lee[3], Young-jin Won[4], Tae Kuk Ko[5]

[1] Korea Electrotechnology Research Institute, Changwon 641-120, Korea
[2] Changwon National University, Changwon 641-773, Korea
[3] LS cable, Gumi 730-708, Korea
[4] Korea Electric Power Corporation, 135-791, Korea
[5] Yonsei University, Seoul 120-749, Korea

Received 24 September 2010; accepted 19 November 2010

***Abstract*-- The renewable energy source is considered as a good measure to cope with the global warming problem and the fossil energy exhaustion. The construction of electric power plant such as an offshore wind farm is rapidly increasing and this trend is expected to be continued during this century. The bulky and long distance power transmission media is essential to support and promote the sustainable expansion of renewable energy source. DC power cable is generally considered as the best solution and the demand for DC electric power has been rapidly increasing. Especially, the high temperature superconducting (HTS) DC cable system begins to make a mark because of its advantages of huge power transmission capacity, low transmission loss and other environmental friendly aspects. Technical contents of DC HTS cable system are very similar to those of AC HTS cable system. However the DC HTS cable can be operated near its critical current if the heat generation is insignificant, while the operating current of AC HTS cable is generally selected at about 50~70% of the critical current because of AC loss. We chose the specifications of the cable core of 'Tres Amigas' project as an example for our study and investigated the heat generation when the DC HTS cable operated near the critical current by some electric and thermal analyses. In this paper, we listed some technical issues on the design of the DC HTS cable core and described the process of the cable core design. And the results of examination on the current capacity, heat generation, harmonic loss and current distribution properties of the DC HTS cable are introduced.**

1. INTRODUCTION

There are three asynchronous grids in the United States. They are East Interconnection, West Interconnection and Electric Reliability Council of Texas (ERCOT). In order to connect these independent grids, a big HTS cable project named as 'Tres Amigas' was initiated by AMSC and Tres Amigas LLC. This project chose the DC HTS cable as a power transmission media since it is more reliable and effective solution over an AC interconnection.

Fig. 1 shows the schematic view of the grid connection of 'Tres Amigas' project and Fig. 2 shows the cross sectional view of an example of DC HTS cable.

The brief specifications of the DC HTS cable are listed in table 1. And we assumed some operating conditions such as table 2, which are arbitrarily selected considering general operating conditions of HTS cable for our study.

* Corresponding author: skedy@keri.re.kr

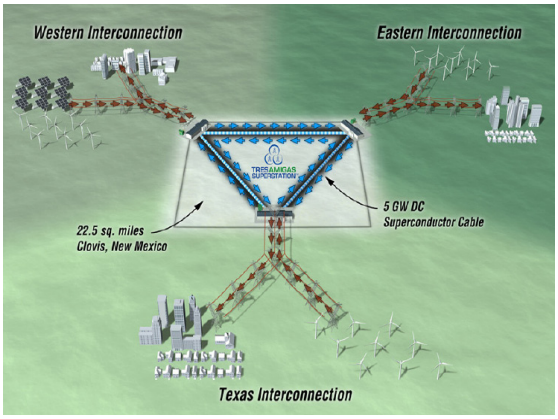

Fig. 1. Schematic view of 'Tres Amigas' project.

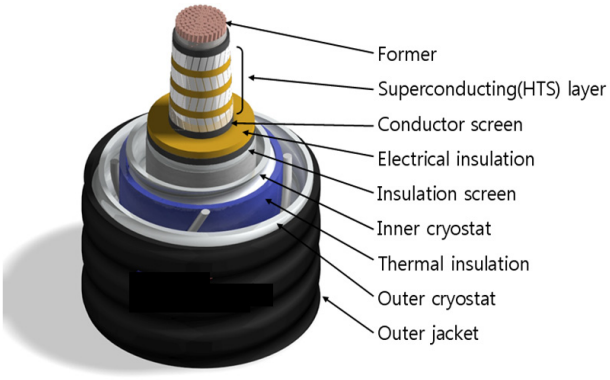

Fig. 2. Cross sectional view of an example of DC HTS cable.

There are several factors are required to design DC HTS cables compared with the AC HTS cables. Following parameters should be considered to design the most economical DC HTS cables.

- Estimation of current capacity
- Heat generation by joint resistance and flux flow
- Current distribution in HTS wires
- Loss generated by DC Harmonics

TABLE I
SPECIFICATIONS OF DC HTS CABLE.

Items	*Values or type*
Length	3.2 km/each side
Nominal voltage	+/- 200 kV DC
Maximum current	12,500 A DC
Maximum power	2.5 GW

TABLE II
SOME ASSUMED OPERATING CONDITIONS FOR OUR STUDY.

Items	*Values*
Operating temperature	65 ~75 K
Minimum operating pressure	5 bar
HTS wire	AMSC 344B, Ic > 80A
Fault current	25 ~ 40 kA, ~1.0 sec

2. DESIGN OF HTS CABLE CORE

2.1. Former

One of the important functions of the former is to bypass the fault current and suppress the temperature rise below the boiling temperature of the LN_2 at operating pressure such as Fig. 3. The heat transfer condition during the fault state can be assumed to be adiabatic because the duration of the fault is too short for the generated heat to transfer through low conductive insulation layer by thermal diffusion. Therefore, the temperature increase of the HTS cable can be calculated with the zero-dimensional adiabatic equation such as (1) [1].

$$C\frac{dT}{dt} = R_f I_t^2 \qquad (1)$$

Where, C is the volumetric heat capacity per unit length of the former (generally commercialized copper), I_t is fault current and T is the temperature of HTS cable. R_f is the resistance of the former, which is varied according to its cross-sectional area.

We investigated the temperature increase of the DC HTS cable for the various fault conditions and calculated the minimum cross-sectional area of the former to satisfy the restriction of the temperature rise at 5 bars as shown in Fig. 4.

At least 400mm^2 of former area meets all of the fault conditions. However, the outer diameter of former must be large enough to lay the number of superconducting wires through which the maximum current (12,500 A) can flow. We selected the former size of 800 mm^2 considering the necessary number of HTS wires. In this case, temperature rise during the fault condition can be restricted much below than boiling temperature of LN_2 and the HTS cable could be continuously operated with the slight temperature increase after fault state. Fig. 5 shows the temperature rise of the HTS cable with the former of 800mm^2 for various fault conditions

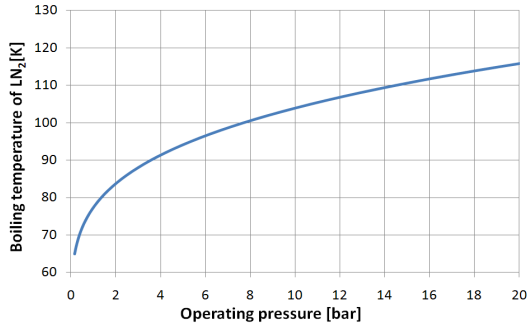

Fig. 3. Boiling temperature of LN_2 according to pressure.

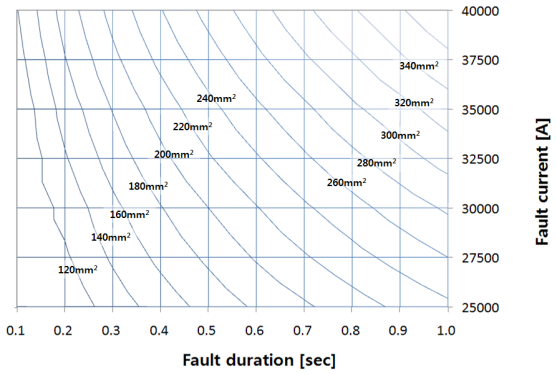

Fig. 4. Minimum cross-sectional area of former to prevent boiling of LN_2 during fault state at 5 bar operation.

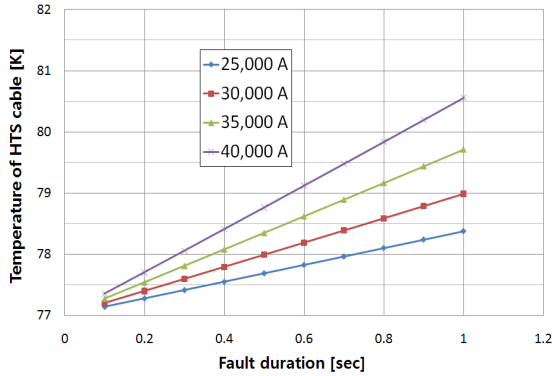

Fig. 5. Temperature rise of the HTS cable with the former of 800mm^2 for various fault conditions.

2.2. Superconducting layers - current capacity

The critical current of the HTS wire sensitively varies depending on the magnetic field and the temperature.

Fig. 6 shows the variation of the critical current of 344B HTS wire depending on the parallel and perpendicular magnetic field at 65 K and 77 K. And we measured the critical current of 344B HTS wire according to the operating temperature as shown in Fig. 7. The critical current increases by 8 % / K in the temperature range of 70 K to 77K. This value was used in the calculation of the temperature dependent critical current of the DC HTS cable.

The generated magnetic field of the HTS cable is smaller than that of other HTS power apparatuses and the critical current of the HTS cable is regarded to mainly depend on

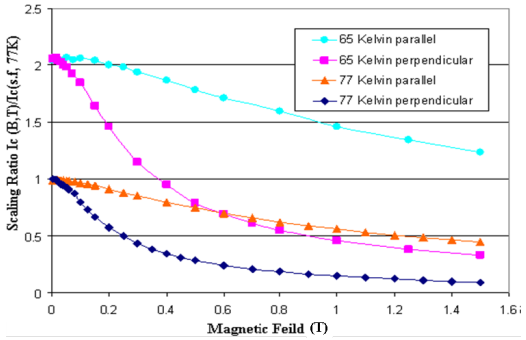

Fig. 6. Temperature and magnetic field dependent critical current of 344B HTS wire [2].

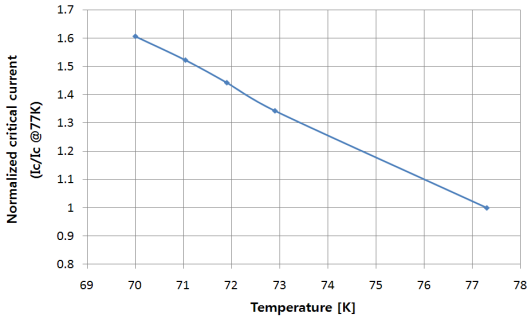

Fig. 7. Normalized critical current of 344B HTS wire according to the temperature.

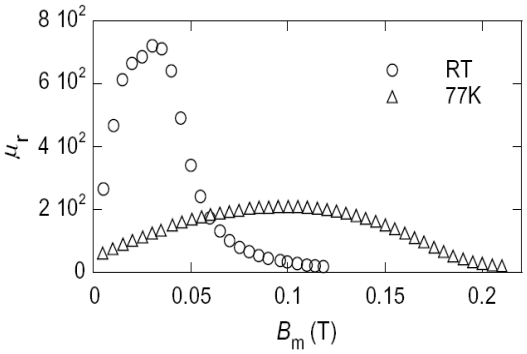

Fig. 8. Magnetic properties of Ni-alloy substrate of 344B HTS wire [3].

the temperature. However, DC HTS cable can be operated near its critical current and a little variation of the critical current by the magnetic field can affect the operation characteristics.

Electro-magnetic field analysis was performed for an example of DC HTS cable which has four superconducting layers of 106 HTS wires in total in order to calculate parallel and perpendicular magnetic field and examine the effect of the magnetic field on the decrease of critical current of DC HTS cable. In addition, the substrate of the 344B HTS wire shows the weak ferro-magnetic property as shown in Fig. 8. The relative permeability of the substrate was also considered in the analysis.

The rated current of each strand must be 117.92 A to meet the maximum operating current of 12,500 A with 106 HTS wires. Fig. 9 shows the calculated magnetic field when the rated current was applied to each wire.

Fig. 10 shows the parallel magnetic field on the HTS wire. The maximum parallel magnetic field over 0.2T seems to be restricted just in the substrate and its effect on the decrease of critical current seems to be negligible. The parallel magnetic field in the superconductor region of the outermost layer is 0.12 T.

Fig. 11 shows the perpendicular magnetic field at the outermost layer along the circumferential direction. The peak of magnetic field is located at the edge of the HTS wire and the average perpendicular magnetic field is about 0.01T for all layers.

Since the perpendicular magnetic field was too weak to make any effect on the decrease of the critical current, the parallel magnetic field was only considered for the estimation of the decreased critical current.

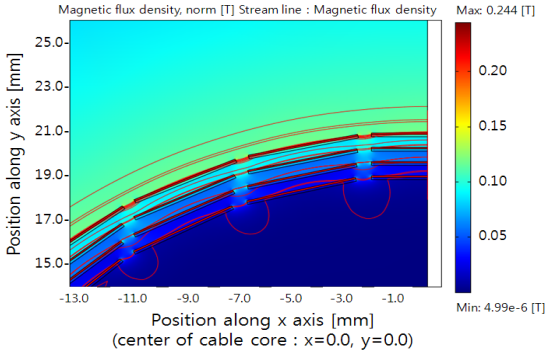

Fig. 9. Calculated magnetic field when the rated current is applied.

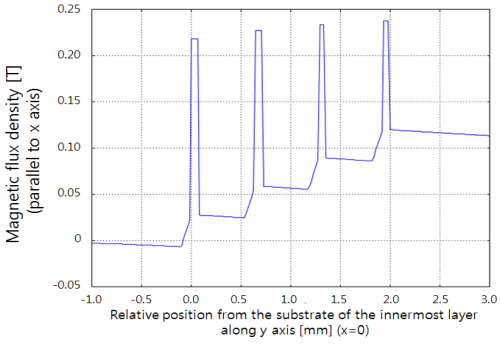

Fig. 10. Parallel magnetic field for all layers.

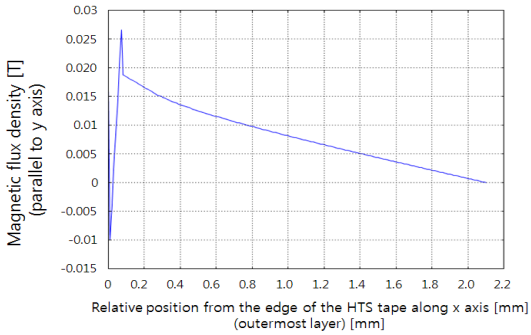

Fig. 11. Perpendicular magnetic field for the outermost conducting layer.

TABLE III
PARALLEL MAGNETIC FIELD OF EACH LAYER AND THE CRITICAL CURRENT DEGRADATION BY THE MAGNETIC FIELD.

Layer	Current/ layer [A]	No. of wires	Current /wire [A]	magnetic field [T]	Ic Degradation [%]
1st	2948	25	117.92	0.03	1.0
2nd	3066	26	117.92	0.06	1.2
3rd	3183	27	117.92	0.08	1.5
4th	3301	28	117.92	0.12	2.4
Total	12,500	106	-	-	-

Table 3 shows the parallel magnetic field on each layer and the degradation of critical current by the applied magnetic field.

We investigated the critical current of DC HTS cable considering the effect of magnetic field and operating temperature. We assumed that the DC HTS cable could be operated at the temperature range of 65 K to 75 K and the critical current of HTS wire is 80 A to 100 A, which is the general value of commercialized 344B HTS wire. Fig. 12 shows the calculated results.

If we use 80 A class HTS wires, the operating temperature must be lower than 71 K in order to keep the critical current of the cable over the maximum operating current (12,500 A). And if the maximum operating temperature is set to 72 K and 90 A class HTS wires are used, the critical current of the cable becomes to be 13,185 A with the operating current margin of 5.5%. We selected this operating condition for the following studies in order to investigate the thermal and current distribution characteristics during the cable operated near its critical current.

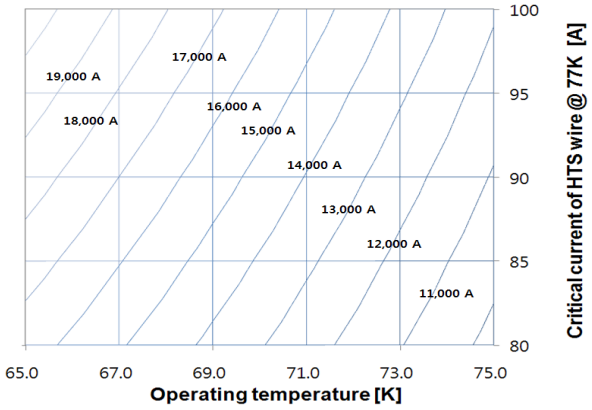

Fig. 12. Critical current of DC HTS cable depending on the operating temperature and the critical current of HTS wire.

3. THERMAL ANALYSIS

3.1. Heat generation by joint resistances

We assumed that single pole of DC HTS cable consists of 2 terminations and 3 joints boxes at every 800m as shown in Fig. 13. And HTS wires are assumed to be spliced at every 100m considering the piece length of HTS wire which can be commecially supplied.

The joint resistance between current lead and HTS wire can be generally controlled less than 100nΩ and the splice resistance between wires at the joint box can be controlled less than 1uΩ considering face to back joint. There are 31 splices along the 3.2 km cable length and the splice resistance is known as less than 150 nΩ .

Table 4 shows the resistivie heat generation considering the parallel resistance of 106 HTS wires at the maximum current of 12,500 A.

Resistive heat generation at the terminations and joints are localized and the heat generation at the splices are distributed along the cable. The estimated overall resistive loss is estimated as 9.36W and this loss is negligigle considering heat invasion from the cryostat.

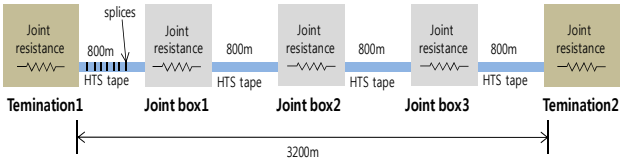

Fig. 13. Connection configuration of 1 pole DC HTS cable.

TABLE IV
JOINT RESISTANCE AND RESISTIVE LOSS.

	Joint resistance /wire [nΩ]	Parallel resistance of HTS tapes [nΩ]	Loss [w]
Termination 1	100	0.94	0.15
Joint box 1~3	1,000	9.43	4.41
Splices (31ea)	3,150	29.71	4.64
Termination 2	100	0.93	0.15
Total loss			9.36

3.2. Flux flow loss

Since the transport current is near the critical current, flux flow loss can be generated in the HTS wire according to the following equation (2).

$$V = E_0 \left(\frac{I_o}{I_c(T)} \right)^n L \qquad (2)$$

Where, V is the voltage drop along the superconducting wire of which critical current is I_c and length is L when operating current (I_o) is applied. I_c is a fuction of temperature (T) as shown in Fig. 7. E_0, and n (index value) are assumed to be 0.1 mV/m (criterion of DC critical current) and 25.

Therefore, the voltage drop appears rapidly as the operating current approaches the critical current and flux flow loss increases.

If the inlet temperature of the cable is fixed to 65 K and the outlet temperature is 72 K. The temperature distribution along the cable can be assumed as in Fig. 14. The critical current varies along the cable according to the temperature variation. Therefore the estimated average critical current of four superconducting layers is 196.7 A and 124.4 A at the inlet and the outlet of the cable as shown in Fig. 14.

The flux flow loss per unit length can be estimated considering the variation of the critical current as shown in Fig. 15. The maximum flux flow loss is 0.327 W/m and it is generated at the outlet of the cable. If the flux flow loss along the cable is integrated, the whole flux flow loss is 84.1 W.

At the outlet of the cable, the largest flux flow loss should be drained across the insulation layer. In this case, the estimated temperature drop across the insulation layer can be 0.3 K.

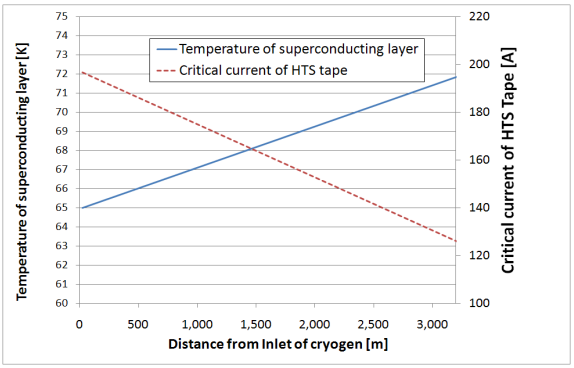

Fig. 14. Temperature and critical current distribution along the cable.

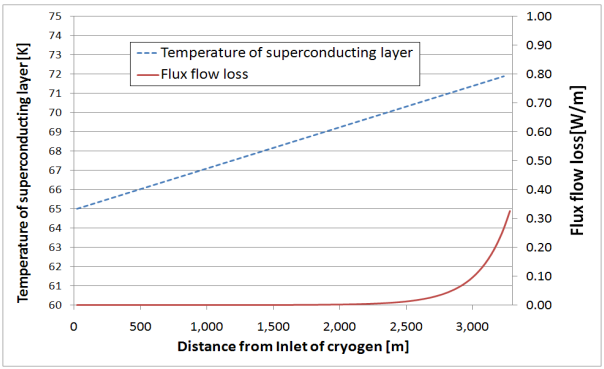

Fig. 15. Flux flow loss distribution along the cable.

4. CURRENT DISTRIBUTION BETWEEN WIRES

In case of DC HTS cable, the current distribution between HTS wires in parallel connection is determined by the resistance ratio among the wires. The resistance components are composed of termination and joint resistance. If severe current imbalance occurs, the flux flow loss can be increased. Therefore, it is needed to investigate the possibility of the current imbalance due to the non-uniform joint resistance of each wire at the termination and joint.

Fig. 16 shows the equivalent circuit diagram for the DC HTS cable. R_{jm} is the sum of splice resistances on each HTS wire and I_m is the transport current at each wire. The HTS wires are not insulated and there would be some electric contacts between adjacent wires represented as R_{cm} in the figure. But the resistances of the contacts are expected to be much higher than those of splices and the flux flow. Therefore, they can be neglected in the calculation.

Equation (3) represents the circuit as shown in Fig. 16. Where, temperature dependent critical current (I_c) along the cable length (L=3200m) such as Fig. 14 was considered to calculate the voltage drop by the flux flow.

Table 5 shows the practical range of the splice resistance for each component. Splice resistance between HTS wires was fixed as 150nΩ and the total transport current (I_t) is 12,500 A. In the analysis, the linear resistance distribution from minimum (4.750 μΩ) to maximum (6.350 uΩ) splice resistance was used. The voltage drop by the flux flow loss was calculated by the sum of the second term of (3) as shown in equation (2).

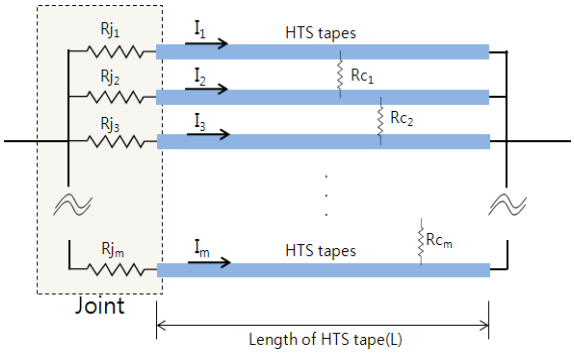

Fig. 16. Equivalent circuit diagram of DC HTS cable.

$$
\begin{aligned}
Rj_1 I_1 + E_0 \sum_{k=1}^{L} \left(\frac{I_1}{I_c(T(k))} \right)^n &= V \\
Rj_2 I_2 + E_0 \sum_{k=1}^{L} \left(\frac{I_2}{I_c(T(k))} \right)^n &= V \\
&\vdots \\
Rj_m I_m + E_0 \sum_{k=1}^{L} \left(\frac{I_m}{I_c(T(k))} \right)^n &= V \\
I_t = \sum_{k=1}^{m} I_k &
\end{aligned}
\tag{3}
$$

TABLE V
PRACTICAL RANGE OF THE JOINT RESISTANCE AT EACH JOINT COMPONENT.

Components	*Joint resistance/wire [nΩ]*	
Termination 1	min	50
	max	100
Joint box 1	min	500
	max	1,000
Joint box 2	min	500
	max	1,000
Joint box 3	min	500
	max	1,000
splices	-	3,150
Termination 2	min	50
	max	100
Total (Rj_m)	min	4,750
	max	6,350

The calculated current distribution varies from 117.88A to 117.96A and the current imbalance seems to be negligible as shown in Fig. 17. In this case, the increased flux flow loss is 92.8 W, which is increased by 8.7 W. This uniform current distribution seems to be resulted from the relatively large resistance by the flux flow loss compared with the joint resistance.

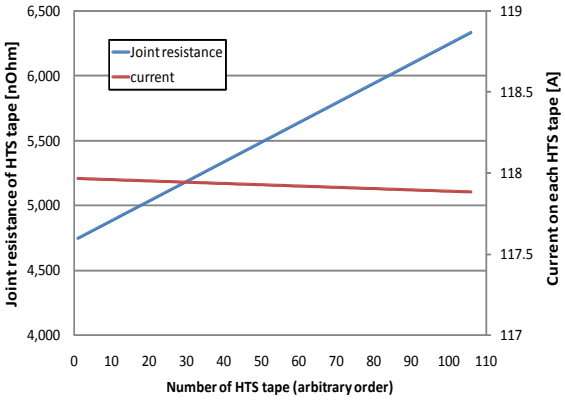

Fig. 17. Splice resistance distribution among the wires and current distribution on each wire.

5. POWER LOSS DUE TO HARMONICS

The voltage source converter (VSC) which is recently used as the power converting component for the DC cable system tends to generate voltage harmonics. The voltage harmonics can induce the high order current ripples on the DC cable. Especially for the DC HTS cable operated near its critical current, the AC loss can be highly increased by the high frequency current ripples.

We investigated the effect of the current harmonics on the AC loss increase of the DC HTS cable using the typical voltage harmonics pattern of the general VSC as shown in Fig. 18 [5, 6].

We assumed that the distance between two poles of DC HTS cable is 5 meters. The inductance and capacitance of the DC HTS cable are calculated based on the design specifications.

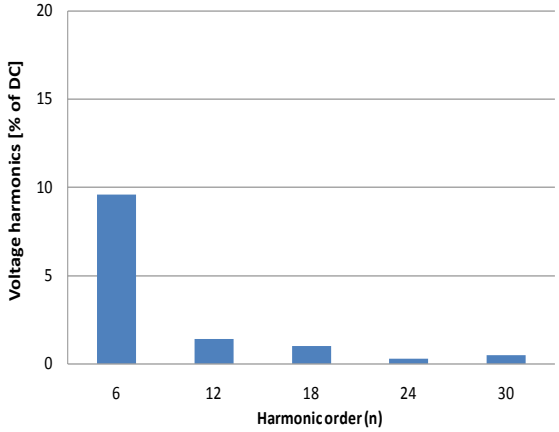

Fig. 18. Typical voltage harmonics of VSC.

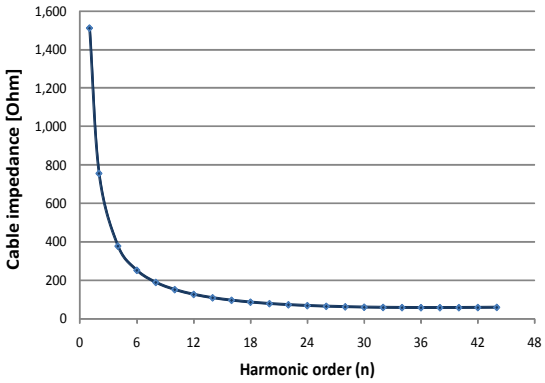

Fig. 19. The impedance of the cable according to the harmonic order (base frequency is 60Hz).

Fig. 19 shows the calculated impedance of the cable according to the harmonic order.

The current ripple of the DC HTS cable can be calculated with the typical voltage harmonics and the cable impedance. And consequently, the AC loss of the cable can be obtained by the equation (4) which represents the AC loss generation of the HTS wires operated near its critical current [4].

Table 6 shows the calculated AC loss. Total AC loss generated by the current ripple is expected to be 1.42 W/m. This value cannot be neglected considering the expected heat loss of the cable cryostat (about 2 W/m).

$$P \cong 4 \cdot 10^{-7} \cdot 2 \cdot \pi \cdot f_n \cdot i_n^{\,2} \qquad (3)$$

Where, I_n is the harmonic current and f_n is frequency of the current.

TABLE VI
AC LOSS GENERATION BY THE HARMONICS OF VSC.

Harmonic order(n)	*Harmonic voltage [V]*	*Harmonic current [A]*	*Impedance [Ohm]*	*AC loss [W/m]*
6	19,200	76.2	252	0.84
12	2,800	22.1	127	0.14
18	2,000	22.9	87	0.22
24	600	8.51	71	0.04
30	1,000	15.6	64	0.17
		Total		1.42

6. CONCLUSIONS

We investigated some key issues on the design of the DC HTS cable core. The effect of magnetic field on the decrease of the critical current was not serious for the case of 12,500A class DC HTS cable. However, for the higher capacity cable over 100,000A which is expected to be developed in near future, this technical issue must be considered more seriously.

The heat generation by the flux flow loss seems to be insignificant from the view of total loss. Therefore, the DC

HTS cable can be operated near the critical current without severe increase of operating cost of the cooling system. However, the flux flow loss at the outlet of cryogen is high enough to make temperature increase at the superconducting layer. The AC loss generated by the current ripple is expected to be very high. Some measures to reduce this AC loss should be devised in the design process of the VSC and power filters.

ACKNOWLEDGMENT

This research was supported by a grant from Center for Applied Superconductivity Technology of the 21st Century Frontier R&D Program funded by the Ministry of Science and Technology, Republic of Korea.

REFERENCES

[1] Seokho Kim, Jae-Ho Kim, Jeonwook Cho, Kideok Sim, Su-Gil Lee, and Hyun-Man Jang, "Investigation on the Stability of HTS Power Cable Under Fault Current Considering Stabilizer," IEEE Transaction on Applied Superconductivity. vol. 17, no. 2, pp 1676-1679, 2007.

[2] Y Jiang, R Pei, Z. Hong, J. Song, F. Fang and T. A. Coombs, "Design and control of a superconducting permanent magnet synchronous motor," *Supercond. Sci. Technol*. vol 20, pp. 585–591, 2007.

[3] D. Miyagi, Y. Yunoki, M. Umabuchi, N. Takahashi, O. Tsukamoto, "Measurement of magnetic properties of Ni-alloy substrate of HTS coated conductor in LN2," *Physica C*, vol. 468, pp. 1743–1746, 2008.

[4] S. Eckroad, "Program on Technology Innovation: a Superconducting DC Cable," *EPRI Report 1020458 ,* 2009.

[5] C. H. Chien, R. W. Bucknall, "Analysis of Harmonics in Subsea Power Transmission Cables Used in VSC–HVDC Transmission Systems Operating Under Steady-State Conditions," *IEEE Transaction on power delivery*, vol. 22, no. 4, pp. 2489-2497, Oct. 2007.

[6] S. Eckroad, "Program on Technology Innovation: Transient Response of a Superconducting DC Long Length Cable System Using Voltage Source Converters," *EPRI Report 1020339 ,* 2009.